University POLITEHNICA of Bucharest
Doctoral School of ELECTRICAL ENGINEERING

DOCTORAL THESIS
- SUMMARY-

PROTECȚIA LA SUPRATENSIUNI A TRANSFORMATOARELOR ELECTRICE DE PUTERE CONECTATE LA LINIILE ELECTRICE DE TRANSPORT A ENERGIEI

OVERVOLTAGE PROTECTION OF ELECTRICAL POWER TRANSFORMERS CONNECTED TO POWER TRANSMISSION LINES

Ph.D. student: Eng. Alina RĂCHIȚEANU
Ph.D. supervisor: Prof. Ph.D. Eng. Constantin GHIȚĂ

Bucharest 2022

CONTENTS

CHAPTER 1
INTRODUCTION

A problem of theoretical and practical interest for high-power electrical transformers and power transmission networks is their behaviour when a voltage pulse is applied to the input terminal of the high-voltage winding of the transformer, also on power transmission lines. The study of transient processes at impulse voltage leads to the correct choice of transformer winding insulation and power line insulation from both a functional and an economic point of view.

1.1. CLASSIFICATION OF OVERVOLTAGES

Depending on their form and duration, overvoltages are divided into the following categories (see also SR EN 60071-1:2006):

a. Temporary overvoltages: These are overvoltages of industrial frequency and relatively long duration. They may be undamped or weakly damped.

b. Transient overvoltages are surges of short duration, not exceeding a few milliseconds. They may or may not be oscillatory. Transient surges fall into several categories:

- slow front overvoltages;
- fast front overvoltages;
- very fast front overvoltages;
- combined overvoltages (transient, slow front, fast front, very fast front).

1.2. NEGATIVE EFFECTS OF LIGHTNING OVERVOLTAGES

Atmospheric overvoltages produce lightning and thunder. Lightning is an electrical discharge between electrically charged clouds and is followed by irregularly shaped glows from interacting clouds. Lightning strikes are electrical discharges between clouds and the earth, and the electrical charges built up in the clouds discharge into the earth.

The greatest lightning strike losses occur when lightning strikes an oil refinery, a flammable substance depot or even an aircraft in the lightning strike zone. The damage caused by lightning strikes is very high and the consequences of lightning fires can lead to the release of toxic gases or other flammable substances, which damage the environment and people in the area.

1.3. BRIEF HISTORY OF THE STUDY OF OVERVOLTAGES PROPAGATION IN ELECTRICAL TRANSFORMERS

Transient regimes related to the propagation of surge waves along the high-voltage winding in electrical transformers cause significant insulation stresses, much higher than the stresses in the nominal regime.

Systematic studies on the phenomenon of overvoltage wave penetration in transformers began in the middle of the second decade of the last century, publications on the differential equation describing winding oscillations, the integral equation of winding oscillations, progressive waves propagating along the transformer winding, the study of surge propagation phenomena in cylindrical transformer windings, new aspects of overvoltage propagation phenomena in transformers with bucket windings and the process of making windings with interleaved (interwoven) coils.

1.4. POWER QUALITY

The quality of electricity is the delivery of this product at standards of excellence. All parameters characterising the electricity must be within acceptable limits. [1] Electricity quality is monitored at every stage of production, transmission, distribution and supply.

Disturbances in the electricity grid such as overvoltages, interruptions, voltage dips, asymmetries, voltage and frequency variations are power quality defects. Meteorological stresses such as lightning strikes, wind, hoar-frost on power equipment introduce the disturbances described above.

1.5. ACKNOWLEDGMENTS

As a sign of gratitude, I would like to thank all those who supported me in carrying out this thesis.

This doctoral thesis was elaborated with the help of the Department of Material Machines and Electrical Drives of the Faculty of Electrical Engineering within the Polytechnic University of Bucharest.

I have the pleasure to give special thanks and a deep gratitude to the professor doctor engineer Constantin GHIŢĂ, the scientific leader of the thesis, for the competent guidance and help brought throughout the realization of this doctoral thesis. At the same time, I also thank the Committee for guiding me for my doctoral activity, which included Prof. PhD. Eng. Tiberiu TUDORACHE, Mr. Assoc. Ion Daniel ILINA and Mr. Assoc. Aurel-Ionuț CHIRILĂ, for the help granted during the period of making the scientific reports related to the doctoral thesis and its final editing.

Some of the results presented in the PhD thesis were obtained with the support of the Human Capital Operational Program, Priority Axis 6 - Education and skills within the project "Development of entrepreneurial skills of PhD and post-PhD students - key to career success" (A-Success) MySMIS code: 125125.

I would also like to thank the Wing Computer Group SRL for supporting my scientific activity in the first part of the doctoral training.

Last but not least, I would like to thank my family for their permanent support and encouragement in order to complete this doctoral thesis.

CHAPTER 2
ELECTRICAL DIAGRAMS OF TRANSFORMERS UNDER OVERVOLTAGE

2.1. INTRODUCTION

Due to the high frequency at which transient overvoltage processes take place, the equivalent schemes valid for normal periodic sinusoidal regimes are no longer valid. The frequency of the lightning overvoltage front is very high (on the order of MHz) and because of this, capacitances appear in the equivalent scheme. On the other hand, for good accuracy, resistances and inductances must also be included in the equivalent scheme.

2.2. EQUIVALENT DIAGRAMS DEFINED WITH PARAMETERS DEFINED PER UNIT LENGTH

A simplified electrical diagram of the overvoltage transformer is shown in Fig. 2.1, which is sufficiently precise for the study. It should be noted that the parameters in the circuit diagram in Fig. 2.1 are parameters defined per unit length, that is defined for each metre of length of the high-voltage winding transformer.

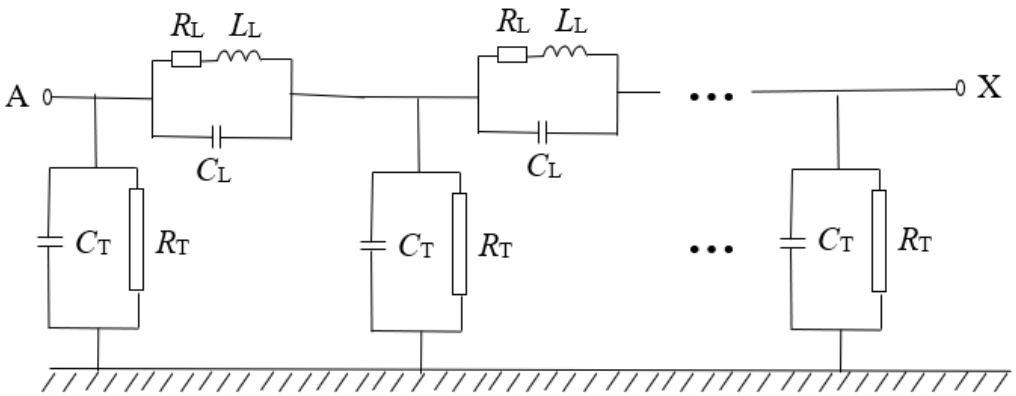

Fig. 2.1. Simplified equivalent electrical diagram of single-phase overvoltage transformer, with parameters defined per unit length

If the equivalent scheme in Fig. 2.1 has a lightning wave applied (at initial time t = 0) to the input terminal A of the high-voltage winding, the value of the voltage u(x, t) can be determined by integrating a differential equation with partial derivatives of order 4 having the form given by the relation [2]:

$$\frac{\partial^4 u}{\partial x^2 \partial t^2} + \frac{R_L}{L_L}\frac{\partial^3 u}{\partial x^2 \partial t} + \frac{1}{C_L L_L}\frac{\partial^2 u}{\partial x^2} - \frac{C_T}{C_L}\frac{\partial^2 u}{\partial t^2} + \left(\frac{R_L C_T}{C_L L_L} + \frac{1}{R_T C_L}\right)\frac{\partial u}{\partial t} - \frac{R_L u}{R_T C_L L_L} = 0 \quad (2.1)$$

where L_L, C_L, R_L, C_T, R_T are parameters defined per unit length measured in [H/m], [F/m], [Ω/m], and x is the measured distance from terminal A to the current point in the high voltage winding and t is the measured time from the moment the lightning wave enters the input terminal A of the high voltage winding. The values of the parameters appearing in equation (2.1) are values defined per unit length.

2.3. ELECTRICAL DIAGRAMS DEFINED WITH LUMPED PARAMETERS EXPRESSED IN ABSOLUTE VALUES

In this thesis we will work with the simplified electrical diagram in Fig. 2.2 where the equivalent overvoltage diagram of the single-phase transformer with lumped parameters expressed in absolute values is shown. The input terminals of the 6 winding sections are noted with A_1, A_2, … , A_6. The values of the parameters of the 6 sections are chosen for a low power electrical transformer with an apparent power of 1 kVA. These values will hereafter be called reference values and are as follows [3]: R_{0L} = 2 Ω, R_{0T} = 2000 MΩ, L_{0L} = 2 mH, C_{0L} = 2.2 nF, C_{0T} = 5.5 nF.

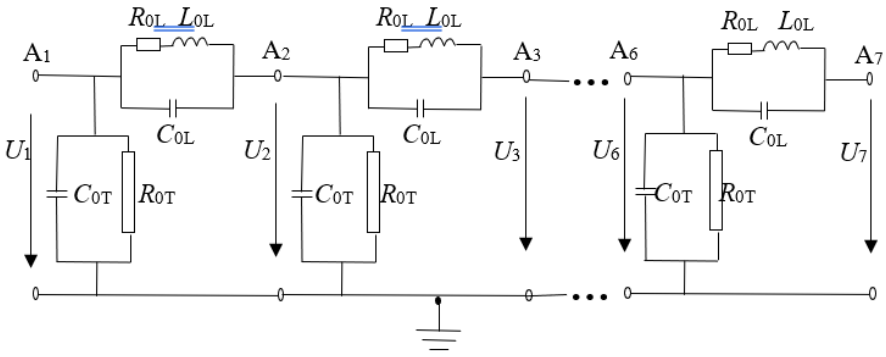

Fig. 2.2. Equivalent diagram at overvoltages with the parameters of the 6 sections having the reference values

The equivalent diagram shown in Fig. 2.2 has been deduced under the following simplifying assumptions:

- Only six transformer winding sections were chosen and in this case, the study of the spatial distribution of the overvoltages leads to some errors. If the number of sections is double it is obvious that the study of the spatial distribution of the overvoltage is closer to reality;

- The six sections into which the winding was divided have the same parameters, ignoring the change in the parameters of the input section A_1 due to the reinforced insulation of its turns;

- It is assumed that the transformer windings are not provided with a guard ring and protective shields connected to the winding input terminals, which will be taken into account when studying the influence of these elements separately in the following chapters of the thesis.

CHAPTER 3
LIGHTNING IMPULSE MODELLING FOR TRANSFORMER WINDING TESTING

3.1. LIGHTNING IMPULSE VOLTAGE WAVEFORM

In this chapter, the determination of the parameters of a pulse generator that creates an overvoltage waveform as close as possible to the waveform presented in IEC 60060 - 1 [4] and IEC 60060 - 2 [5] is considered. Starting from the equivalent diagrams of the electrical transformer exposed to overvoltages, the overvoltage waves produced by the impulse

generator are applied to these equivalent diagrams and the propagation of the overvoltage waves along the windings of the transformer, both at the initial moment and at other moments of time, is studied by numerical simulation in the following chapters.

3.2. LIGHTNING IMPULSE VOLTAGE GENERATION

The impulse overvoltage generator is an important part of the transformer test system [6]. Given the very high pulse frequency, the generator also produces disturbances in the measured signal, including oscillations in the wavefront area, especially around the origin, but also in the decreasing wavefront area, here the disturbances have less influence. [7]

A less difficult way of dealing with the problems caused by lightning surges on transformer windings is to replace experimental test methods with numerical simulation methods LTspice (spice - Simulation Program with Integrated Circuit Emphasis) [8]. In this case, no additional disturbances occur in the signal applied to the transformer winding and therefore no special filters are needed. Also in this case, errors due to the simulation process occur, but they have only a quantitative influence so that from a qualitative point of view, the simulated phenomena lead to correct conclusions.

3.3. MODELING THE LIGHTNING IMPULSE VOLTAGE WAVEFORM

The simplified circuit diagram of the pulse generator is shown in Fig. 3.1. This generator was first designed by Erwin Otto Marx [9].

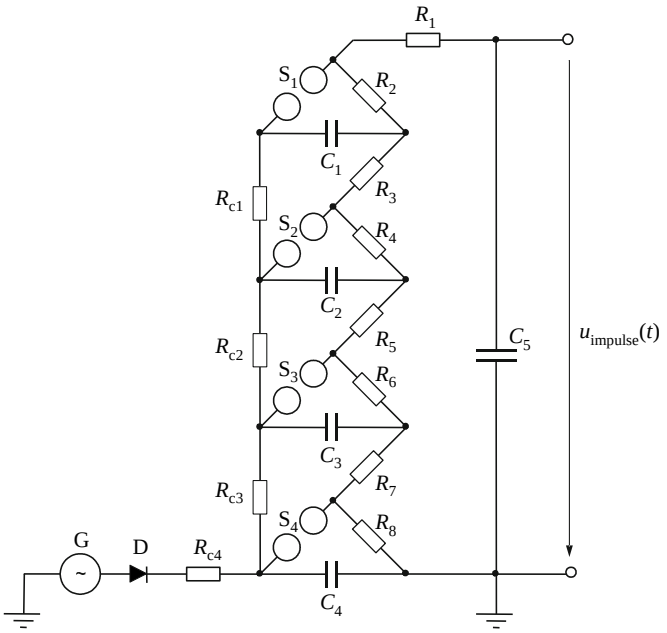

Fig. 3.1. Marx impulse generator with 4-stage generic circuit diagram

3.4. THE SIMULATION CIRCUIT OF THE IMPULSE GENERATOR USING LTSPICE

Based on the pulse generator schematic shown in Fig. 3.1, the LTspice model of the pulse generator shown in Fig. 3.2.

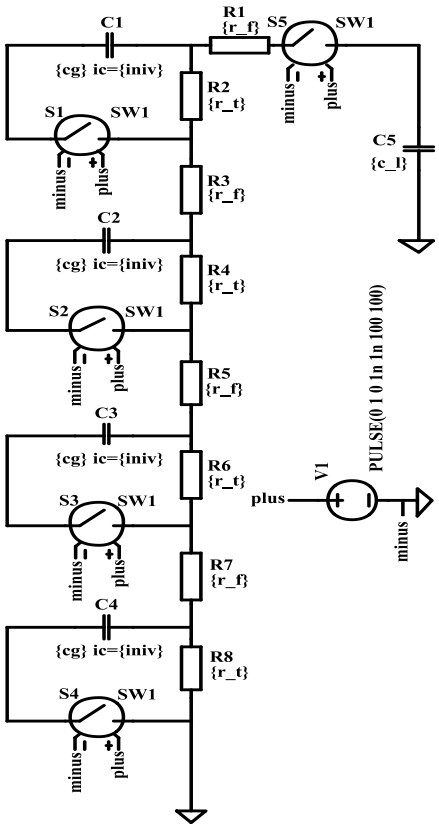

Fig. 3.2. LTspice simulation of impulse over-voltage generator [3]

The charging resistances $R_{c1}...R_{c4}$ are not included in Fig. 3.2, because for the simulation at the initial moment of time, the impulse capacitors C_1, C_2, C_3, C_4, are already defined as charged. This is achieved by using the LTSPICE function, IC (initial condition).

The sphere gaps S_1 … S_4 are replaced with switches that are voltage-controlled. Switch S_5 is added in LTspice circuit in order to prevent the discharge of the impulse capacitors when a large delay is wanted (for example, a delay of 1 s).

The control voltage threshold of the switches is set to 0.5 V. The control voltage is of pulse type with 1 VDC voltage and equal rise and fall times of 1 ns. The simulation is transient type with stop time set to 50 μs, while the maximum simulation time step is 1 ms. The integration method is modified trapezoidal.

Following the simulation, the standard overvoltage waveform, shown in Fig. 3.3, for the case when the pulse generator is in no-load mode of operation. For the per-unit system the value to which the voltage is related is 1 kV.

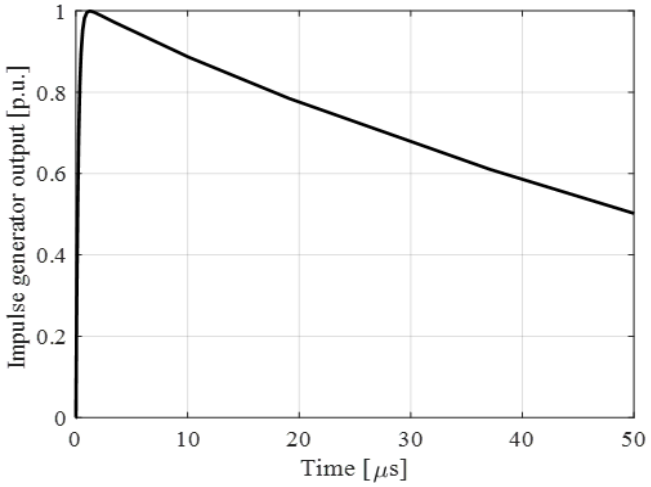

Fig.3.3. The standard waveform shape of lightning impulse simulated in LTspice

There is consistency between the standard waveform and the SIMULATION waveform, as the rising wavefront reaches a maximum value of 1 kV at 1.255 μs (falling within the standard error limits), and the end part (tail part) returns to 0.5 kV within 50 μs.

CHAPTER 4
SIMULATION OF LIGHTNING IMPULSE PROPAGATION IN TRANSFORMER WINDING USING LTSPICE

4.1. INTRODUCTION

After the waveform has been generated using the LTspice pulse generator, a transformer with the following characteristics shown in Tab.4.1 will be chosen for simulation.

Tab.4.1. Technical data of the transformer

Name	Value
Product type	Isolation and safety transformer
Rated power	1 kVA
Input voltage	230 V a.c. single phase , terminals: N-L1 400 V a.c. phase to phase , terminals: L1-L2
Output voltage	115 V a.c.
Secondary winding	Single

Input voltage limits	207...253 V 360...440 V
Frequency limits	47…63 Hz
Input voltage tolerance	+/- 15 V
Efficiency	94 %
Power dissipation in W	63,8 W
Continuous output overvoltage	3 % (no load, warm state)
Maximum voltage drop at nominal load	0,5 %
No-load losses	26,5 W
Short circuit voltage	0,0304
Output protection type	Overload protection Overvoltage protection Short circuit protection
Dielectric strength	2000 V between winding and ground 4000 V between primary and secondary

The transformer on which the simulations are performed has the high voltage winding divided into six identical sections, as shown in the equivalent diagram in Fig. 2.2.

4.2. EQUIVALENT TRANSFORMER CIRCUIT DIAGRAM SIMULATED IN LTSPICE

Fig.4.1 shows the LTspice implementation of the full equivalent transformer circuit when an overvoltage waveform is applied to the transformer. The seven terminals can be seen (A_1 … A_7) and the resulting six identical sections (S_1 … S_6), which are connected in series.

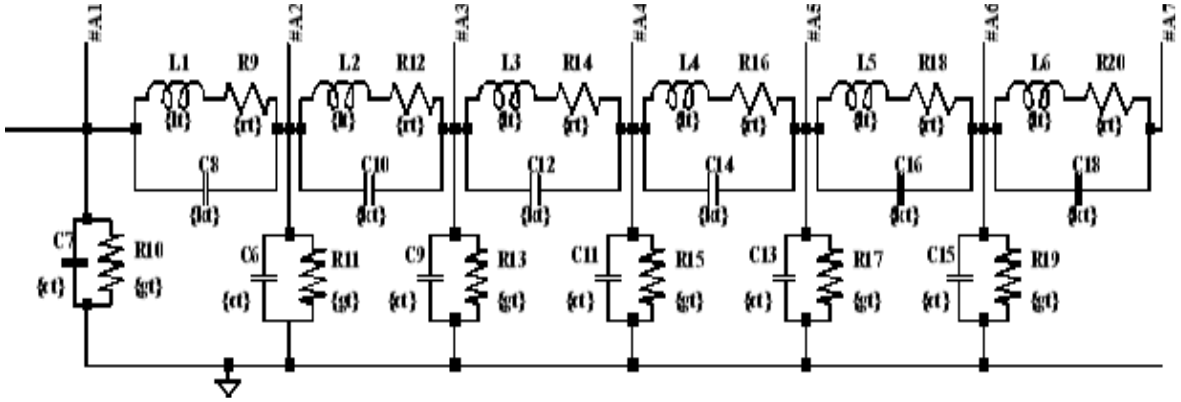

Fig. 4.1. Equivalent transformer circuit diagram using the lumped parameter model and implemented in LTspice software

The case study analysed considers the winding end terminal (A_7) as unconnected to ground.

4.3. SIMULATION OF LIGHTNING IMPULSE PROPAGATION IN THE TRANSFORMER HIGH VOLTAGE WINDING

The resulting propagation in time and space of the applied overvoltage is shown in Fig. 4.2 for the first four terminals (A_1, A_2, A_3, A_4) and in Fig. 4.3 for the last three terminals (A_5, A_6, A_7). In these figures, overvoltage values are expressed in relative units and time is expressed in μs.

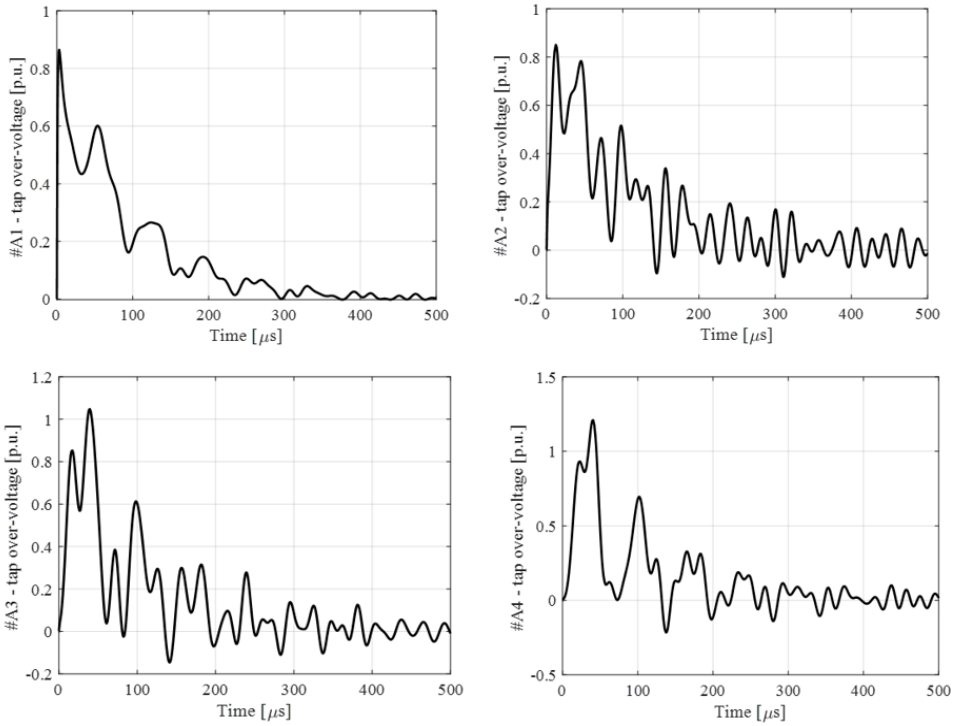

Fig. 4.2. Propagation in time and space of the impulse overvoltage for the first four terminals (A_1, A_2, A_3, A_4) [3]

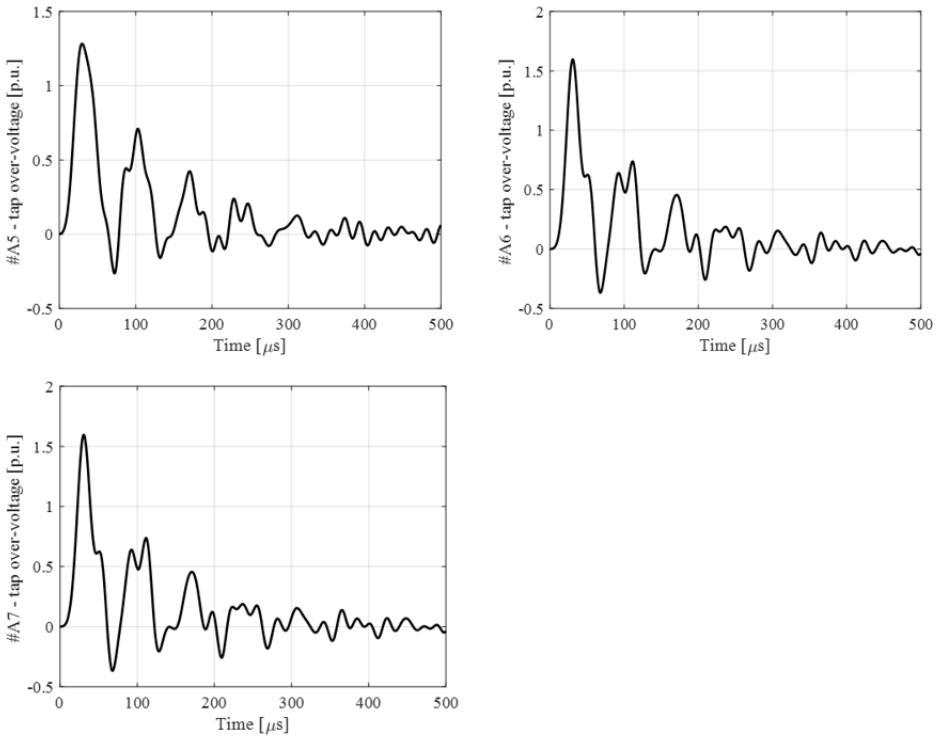

Fig. 4.3. Propagation in time and space of the impulse overvoltage, for the last three terminals (A_5, A_6, A_7) [3]

The most stressed section is the last one (terminals A_6 - A_7), because the surge reaches 1.6 kV after 30 μs. Observing the overvoltage variation shapes in Fig. 4.2 and Fig. 4.3, the general conclusion is that the overvoltage values decrease with time. After the time of 500 μs, the peak value of the measured voltage waves is less than 10 percent of the initial value at all 6 terminals.

The simulations carried out in this chapter are general because the values of the overvoltages propagating along the high voltage winding are measured in relative units.

CHAPTER 5

INFLUENCE OF VARIATION OF EQUIVALENT DIAGRAM PARAMETERS ON OVERVOLTAGE WAVE PROPAGATION

5.1. INTRODUCTION

Particular attention must be paid to the insulation system of the high-voltage windings of the transformer, which must withstand these lightning voltages, and to special elements to mitigate the effects of these overvoltages.

5.2. SPATIAL AND TEMPORAL DISTRIBUTION OF THE OVERVOLTAGE WAVE

To begin with, the reference values of the parameters of the equivalent overvoltage scheme, denoted by 'zero', shall be taken as follows: R_{0L} = 2 Ω, R_{0T} = 2000 MΩ, L_{0L} = 2 mH, C_{0L} = 2.2 nF, C_{0T} = 5.5 nF. The values of these parameters are the same for all 6 sections of the transformer high voltage winding.

A standard voltage pulse, whose peak value is U100 = 1 kV, is applied to the input terminal of the transformer. Model in LTspice the time and space propagation of the overvoltage wave for the above reference values of the equivalent scheme parameters and obtain the curves in Fig. 5.1. [10]

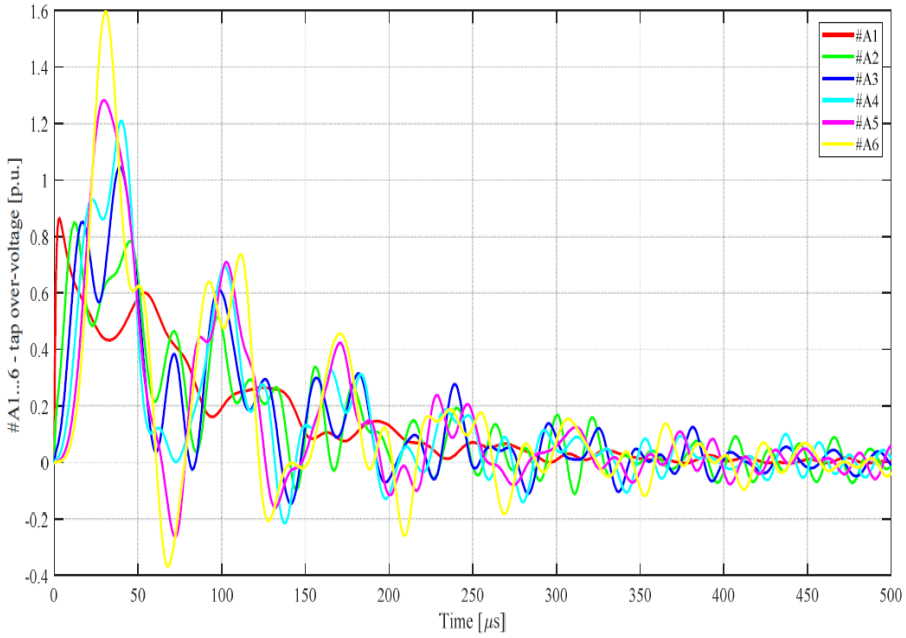

Fig. 5.1. Time variation curves of the overvoltages propagated along the high voltage winding, simulated for the input terminals of the 6 sections. The colour legend of the curves is as follows: terminal A_1 - red; terminal A_2 - green; terminal A_3 – dark blue; terminal A_4 - light blue; terminal A_5 - magenta; terminal A_6 - yellow.

By observing the shapes of the time variation curves of the overvoltage propagation along the high voltage winding, some important conclusions can be deduced:

- Although the maximum value of the overvoltage at the input of the high voltage winding is 1 kV it is found that through propagation, the maximum value of the overvoltage is lower or higher than its value at the input. Thus for terminal A_1 the maximum voltage value is 861 V, for terminal A_2 the maximum value is 850 V, for terminal A_3 the

maximum value is 852 V, for terminal A_4 the maximum value is 1209 V, for terminal A_5 the maximum value is 1282 V and for terminal A_6 the maximum value is 1541 V. The maximum overvoltage measured at any one terminal of the winding may be the first maximum in time (terminals A_1, A_2, A_5, A_6) or the second maximum in time (terminals A_3 and A_4), as shown by the curves in Fig. 5.1.

- Whether it is the first maximum or the second maximum, only the maximum value of the voltage for a given terminal of the high voltage winding will be considered in the rest of the study.
- The most dangerous voltage peaks are obtained approximately within the first 40 μs after the overvoltage wave penetrates the input terminal of the high-voltage winding. After 350 μs the value of the maximum overvoltage drops to about 10% of the most dangerous maximum, obtained at terminal A_6, about 30 μs after the wave penetration into the transformer.

5.3. INFLUENCE OF VARIATION OF EQUIVALENT DIAGRAM PARAMETERS ON OVERVOLTAGE WAVE PROPAGATION

Starting from the reference values of the parameters of the equivalent diagram R_{0L}, R_{0T}, L_{0L}, C_{0L} şi C_{0T}, the influence of the variation of each of the five parameters of the equivalent diagram is studied one by one by modelling in LTspice under the following scenario: one parameter is varied, the other four remain constant at their reference values. Then another parameter is varied, the other four also remaining constant at their reference values, and the process is continued three more times. In this way, the influence of each of these parameters on the maximum values of the overvoltages occurring along the high voltage winding of the transformer is studied in turn.

Case 1. Influence of the variation of the longitudinal capacitance C_L

The influence of the longitudinal capacitance C_L, n the maximum values of the voltages propagating along the winding, for all 6 input terminals A_1, A_2, ... , A_6 of the equivalent diagram is studied. The modelling procedure is as follows:

Choose, for example, 10 values for the longitudinal capacitance C_L, n relation to the reference value C_{0L}, which are given in Tab. 5.1, the rest of the values of the other 4 parameters, for each of the 10 values of capacitance C_L, emain constant and equal to their reference values: R_{0L} = 2 Ω, R_{0T} = 2000 MΩ, L_{0L} = 2 mH, C_{0T} = 5.5 nF.

Tab. 5.1 C_L longitudinal capacitance values for which simulations are performed

Value of C_L	$0.4C_{0L}$ = 0.88 nF	$0.6\ C_{0L}$ = 1.32 nF	$0.8\ C_{0L}$ = 1.76 nF	C_{0L} = 2.20 nF	$1.2\ C_{0L}$ = 2.64 nF	$1.4C_{0L}$ = 3.08 nF	$1.6C_{0L}$ = 3.52 nF	$1.8C_{0L}$ = 3.96 nF	$2C_{0L}$ = 4.4 nF	$4\ C_{0L}$ = 8.8 nF

For the 10 values of the longitudinal capacitance the same standard overvoltage wave with a maximum front of 1 kV is applied to the input terminal of the transformer. For each individual case, the maximum value obtained for the voltage propagating along the winding is determined. The values of these maxima are given in Tab. 5.2, for each of the 10 values of the longitudinal capacitance and for each of the 6 terminals of the equivalent scheme. Only the maximum values are taken into account because they are the most dangerous for the high voltage winding.

In Fig. 5.2 show the graphs of the maximum voltages as a function of the value of the longitudinal capacitance C_L, for terminals A_1, A_2, ... , A_6.

For example, for the longitudinal capacitance value of 0.88 nF, the first voltage maximum occurs at terminal A_6, and has a value of 1659.3 V, a value about 66% higher than the overvoltage value at the winding input, which was 1 kV. It is also found that terminal A_6 is the most stressed for all 10 values of longitudinal capacitance. Another finding is that as the C_L longitudinal capacitance increases, the value of the first maximum at terminal A_6 decreases. Thus if the value of the longitudinal capacitance increases from the value of 0.88 nF to the value of 8.8 nF, the value of the highest voltage maximum, corresponding to terminal A6, decreases by about 16.39 %.

Tab. 5.2 Maximum voltage values as a function of longitudinal capacitance variation C_L

Value of C_L	The values in [V] of the maximum U_{max} calculated at the terminals A_1, A_2, A_3, A_4, A_5, A_6					
	A_1	A_2	A_3	A_4	A_5	A_6
$0.4\ C_{0L}$ = 0.88 nF	869.50	874.90	883.03	908.38	1290.9	**1659.3**
$0.6\ C_{0L}$ = 1.32 nF	861.45	863.37	871.56	912.44	1242.0	1541.8
$0.8\ C_{0L}$ = 1.76 nF	861.45	858.40	861.63	921.58	1266.7	1541.8
C_{0L} = 2.20 nF	861.45	850.76	852.33	931.84	1282.6	1561.8
$1.2\ C_{0L}$ = 2,64 nF	861.45	841.84	846.67	945.11	1291.1	1543.8
$1.4\ C_{0L}$ = 3.08 nF	860.24	832.93	843.44	957.12	1296.1	1527.7
$1.6\ C_{0L}$ = 3.52 nF	861.45	824.53	841.94	968.70	1297.2	1520.8
$1.8\ C_{0L}$ =3.96 nF	860.24	816.61	839.71	979.39	1298.1	1515.7
$2\ C_{0L}$ = 4.4 nF	859.03	809.16	837.61	988.93	1278.8	1512.2
$4\ C_{0L}$ = 8.8 nF	847.12	756.10	841.38	1025.1	1250.0	**1387.0**

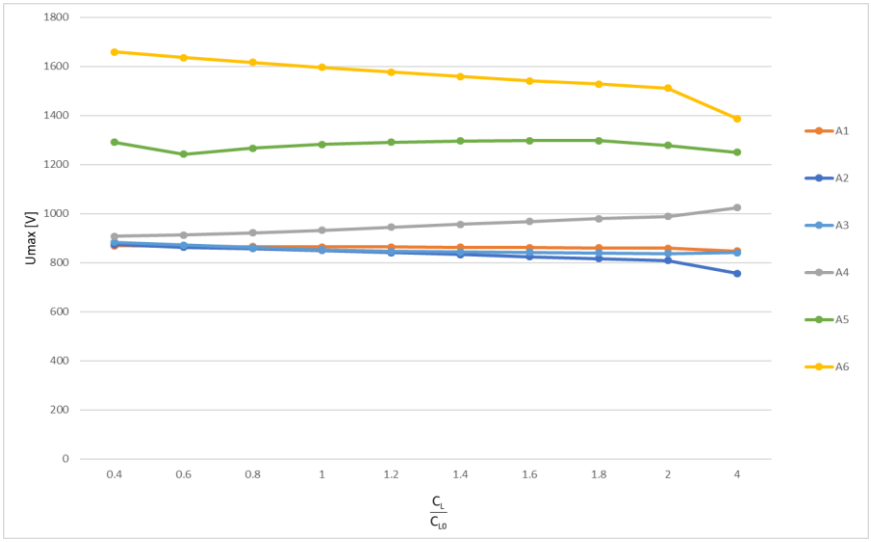

Fig. 5.2. Charts $U_{max}= f\,(C_L)$ | for R_{0L} , R_{0T} , $L_{0L,}$ C_{0T}, at the terminals A_1, A_2 , ... , A_6

Similar to the first case, cases II, III and IV are also analysed, that is, the influence of transverse capacitance C_T, transverse resistance R_T, longitudinal resistance R_L and longitudinal inductance L_L on the maximum values of the voltage propagating along the high voltage winding is studied for all 6 input terminals A_1, A_2, ..., A_6 of the equivalent scheme.

Conclusions

The most stressed part of the transformer high voltage winding is the last section of the winding, with input terminal A_6. Of the five parameters appearing in the equivalent diagram, the highest importance is given to the values of the transverse capacitance C_T and the longitudinal capacitance C_L. Thus, if the value of the transverse capacitance increases from 2.2 nF to 22 nF, the maximum overvoltage value at terminal A_6 decreases by 37.7%. Similarly, if the value of the longitudinal capacitance increases from 0.88 nF to 8.8 nF, the maximum overvoltage value at terminal A_6 decreases by 16.39%. Of less importance are the parameters R_L, L_L and R_T in the equivalent diagram. Similarly, if these 3 parameters vary in the range from 1 to 10, the overvoltage decreases also occur at terminal A_6 and are 3.42 %, 3.07 % and 0.11 % respectively. Thus, the greatest influence on the maximum overvoltage value is had by the transverse capacitance C_T and the least influence by the transverse resistance R_T.

CHAPTER 6
INTERNAL PROTECTION OF TRANSFORMERS USING THE GUARD RING AND PROTECTIVE SHIELD

6.1. INTRODUCTION

Electrical discharges caused by lightning cause serious damage to power station equipment, wind farms [11] and the lines connected to them.

In this chapter the proposed solutions are indoor, by constructive methods in the high voltage transformer winding as follows [12] :

a) Use of a guard ring representing an interrupted circular spiral;
b) Use of a sectioned clindrical shield after the generators in order not to form a short-circuit spiral;
c) Bucket windings and the process of making windings with interleaved (interwoven) coils. [13];
d) Reinforcing the input insulation of the high voltage winding for the first 5 to 10% of its turns.

The first two cases (a and b) of internal protection of the transformer high voltage winding are considered in turn below.

6.2. THE INFLUENCE OF THE GUARD RING ON THE OVERVOLTAGE DISTRIBUTION ALONG THE WINDING

Consider the situation where the transformer is fitted with a guard ring only and the protective shield is missing. In this case, the influence of the guard ring on the equivalent transformer diagram is studied. In order to take into account the presence of the guard ring on the equivalent diagram, it is considered that it introduces into the equivalent diagram, at overvoltages, 6 capacitances C_{1G}, C_{2G}, … , C_{6G} corresponding to the 6 sections of the high voltage winding. It is assumed that the values of these capacitances are different for the 6 sections of the high-voltage winding, the highest value being associated with the section at the entrance of the winding and the lowest value being associated with the last section at the end of the high-voltage winding [12].

In Fig. 6.1 shows the equivalent transformer diagram considering that the transformer is provided only with a guard ring and not with a shield.

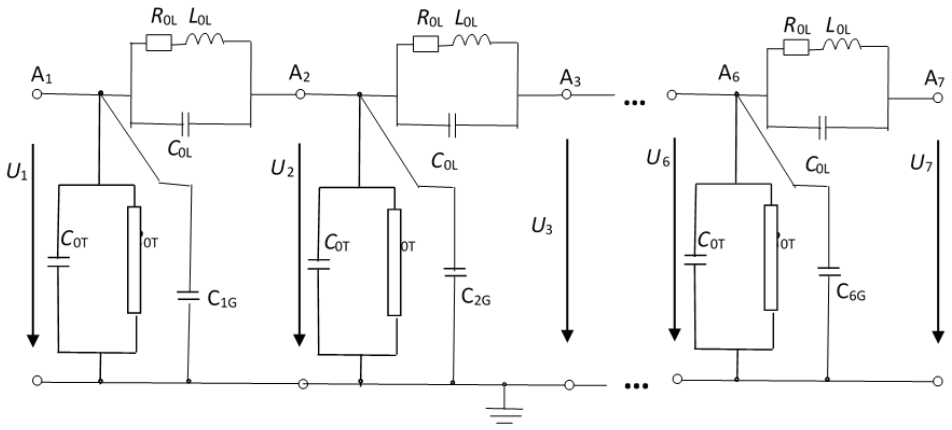

Fig. 6.1. Equivalent diagram of the overvoltage transformer with the guard ring [12]

It is assumed that the 6 capacitances, characteristic of the guard ring, corresponding to the equivalent scheme in Fig. 6.1 will be simulated according to the following four cases, where the values of the capacitances C_{1G}, C_{2G}, … , C_{6G} are those in Tab. 6.1.

For case II and case III the guard ring is considered to introduce into the equivalent diagram a capacitance only in the input section of the high voltage winding, and for case I and case IV the guard ring introduces capacitances in all 6 sections of the winding, with decreasing values on the 6 sections. In all LTspice simulations that are done in the 4 cases the reference values of the 5 parameters of the equivalent scheme are considered: C_{0L} = 2.2 nF, C_{0T} = 5.5 nF, R_{0L} = 2 Ω, R_{0T} = 2000 MΩ, L_{0L} = 2 mH.

For each of the 4 cases, the time variation curves of the overvoltages propagated along the high voltage winding are determined in LTspice.

Influence of the guard ring in the 4 cases

For the 6 values of the guard ring capacitances, a standard overvoltage wave with a maximum front of 1 kV is applied to the input terminal of the transformer. For the 4 cases studied the values of the capacitances are chosen C_{1G}, C_{2G}, … , C_{6G} are those in Tab. 6.1.

Tab. 6.1. Values of capacitances C_{1G}, C_{2G}, … , C_{6G} corresponding to the 4 cases

	Case I	Case II	Case III	Case IV
Capacitance parameter values C_{1G}, C_{2G}, … , C_{6G}	C_{1G} =10 nF	C_{1G} =10 nF	C_{1G} =20 nF	C_{1G} =20 nF
	$C_{2G} = C_{1G}/2$ nF	C_{2G} = 0 nF	C_{2G} = 0 nF	$C_{2G} = C_{1G}/2$ nF
	$C_{3G} = C_{1G}/3$ nF	C_{3G} = 0 nF	C_{3G} = 0 nF	$C_{3G} = C_{1G}/3$ nF
	$C_{4G} = C_{1G}/4$ nF	C_{4G} = 0 nF	C_{4G} = 0 nF	$C_{4G} = C_{1G}/4$ nF
	$C_{5G} = C_{1G}/5$ nF	C_{5G} = 0 nF	C_{5G} = 0 nF	$C_{5G} = C_{1G}/5$ nF
	$C_{6G} = C_{1G}/6$ nF	C_{6G} = 0 nF	C_{6G} = 0 nF	$C_{6G} = C_{1G}/6$ nF

This hypothesis assumes that the values of the capacitances in the equivalent scheme corresponding to the guard ring have a linear decrease for cases I and IV and for cases II and III have a non-zero value only for the input section of the high voltage winding.

Similarly to the simulations carried out in Chapter 5, the simulations are repeated in the LTspice calculation program and the propagation in time and space of the same 1 kV overvoltage wave applied to the input terminal of the high-voltage winding, which was also used to determine the characteristics shown in Fig. 5.1. In this new situation, for example for case I, the curves shown in Fig. 6.2 [12].

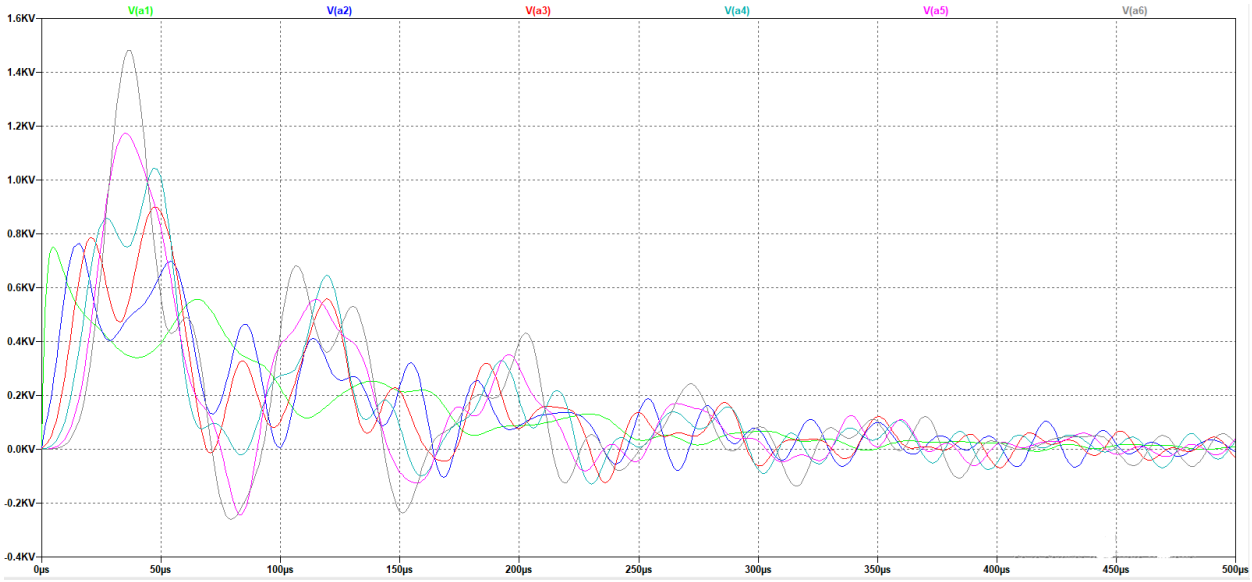

Fig. 6.2. Case I. Time variation curves of the overvoltages propagated along the high voltage winding, simulated for the input terminals of the 6 sections, considering the electrical scheme shown in Fig. 6.1. The colour legend of the curves is as follows: terminal A_1 - green colour; terminal A_2 – dark blue colour; terminal A_3 - red colour; terminal A_4 - light blue colour; terminal A_5 - magenta colour; terminal A_6 - black colour [12].

The guard ring leads to a decrease in the peaks of all overvoltage waves corresponding to the 6 sections of the high-voltage wiring, with values between (7.15 ... 14.30)%. Thus, the reductions of the highest maxima in the 6 sections of the high voltage winding due to the presence of the guard ring are shown in Tab. 6.2, also for case I.

Tab. 6.2. Percentage values of reduction of maxima due to the presence of the guard ring (Case I)

High-voltage winding section	Maximum section overvoltage wave without guard ring	Maximum section overvoltage wave with guard ring	Percentage reduction of maximum due to guard ring
A_1	0.86 kV	0.75 kV	13.09 %
A_2	0.85 kV	0.76 kV	10.09 %
A_3	1.04 kV	0.89 kV	14.30 %
A_4	1.20 kV	1.04 kV	13.82 %
A_5	1.28 kV	1.17 kV	8.58 %
A_6	1.59 kV	1.48 kV	7.15 %

The introduction of the guard ring also has a small influence on the propagation speed of the overvoltage wave along the high voltage wiring. Thus, comparing the curves in Fig. 5.1 (without guard ring) with those in Fig.6.2 (with guard ring), it can be seen that the presence of the guard ring leads to an increase of the overvoltage propagation speed along the winding by about 3.73%.

Influence of the guard ring in case II

Similar to the previous case for the capacitance value C_{1G} the value of 10 nF is chosen and the other capacitances being considered null, the maximum voltage value is 1510 V at terminal A_6, a value 5.35% lower than the overvoltage value at the transformer winding input without additional protection. It is also found that the largest reduction in the overvoltage value is at terminal A_1, by 11.87%.

Influence of the guard ring in case III

In the same way, as in case II, it is found that if the value of capacitance C_{1G} increases from the value of 10 nF to the value of 20 nF, the value of the highest voltage maximum is corresponding to terminal A_6. The decrease of the maximum of the overvoltage waveform most significantly occurs at terminal A_1 by 20.33% .

Influence of the guard ring in case IV

The conclusions that can be deduced from the study of the fourth case are qualitatively similar to those of case I. Similarly, the voltage maximum also occurs at terminal A_6, and has the value of 1370 V, a value 14.14% lower than the value of the transformer voltage maximum without guard ring.

Also similar to the simulations in Case I, the largest percentage decrease in the voltage maximum due to the guard ring is at terminal A_3.

Finally, it can be concluded that the guard ring used as a means of overvoltage protection of electrical transformers is important, as it leads to the reduction of the

overvoltage peaks propagating along the high voltage winding of these transformers. The higher the capacitance of the guard ring, the greater the reduction of overvoltage peaks.

6.3. DETERMINATION OF THE OVERVOLTAGE PROTECTION SHIELD CAPACITANCE FOR THE ELECTRICAL TRANSFORMER

6.3.1. DESCRIPTION OF THE TRANSFORMER USED IN THE SIMULATION

The electrical transformer on which the numerical models of the protective shield is made by the Societatea Comercială Electrotehnica from Bucharest. It is a single-phase, two-column transformer with a power of 2.5 kVA, with a nominal high voltage of 220 V and a nominal low voltage of 110 V. The useful iron cross-section of one column of the magnetic core is S = 33.6 cm2. The height of the transformer window is 150 mm and its width is 50 mm. Both the high voltage winding and the low voltage winding are each made of two coils, placed on the two columns, with coils in series for each of the two windings. [14].

In terms of dielectric properties, it is assumed that the area within the transformer window, the ferromagnetic core area and the area outside the transformer have relative electrical permittivity equal to unity. Under this assumption, some error is made because the areas where the windings are located contain insulating foils that provide insulation between the layers of the two windings as well as insulation between the windings and from outside the windings.

The width of the transformer window is 50 mm. The equivalent thickness of all the insulation in the window is only 4 % of the window width. This means that in practice, if the relative permittivity of the insulation between the layers is taken as unity, this assumption leads to a relatively small error when calculating the capacitance of the screen, without taking into account the insulations in the window. Finally, the final numerically determined capacitance value can be corrected by a correction factor that takes into account the equivalent 2 mm thickness of the transformer window insulation.

6.3.2. DETERMINATION OF THE CAPACITANCE OF THE PROTECTIVE SHIELD BY NUMERICAL METHODS

The electrical transformer has two coils on each column for both high voltage and low voltage winding, the two coils being additionally wound for each winding. A cylindrical protective shield is placed between the coils belonging to the high and low voltage windings

on each column, each shield being sectioned after a generator so as not to form a short-circuit spiral.

The capacitance of the protective shield shall be determined on the assumption that there is only one shield in the window, that is the shield between the high-voltage and low-voltage winding on a single transformer column. This leads to a reduction of the calculation time, without influencing the final result.

Fig. 6.3 shows a diagram of the magnetic core of the transformer with only the shield shown. The determination of the capacitance of this screen are performed using COMSOL [15], which is a simulation software based on advanced numerical methods. The numerical simulation will be done assuming that the relative electrical permittivity of all the environment around the screen is equal to unity. The systematic calculation error that is made is that for the equivalent thickness of all the insulations in the window, representing 4 % of the window width, the relative permittivity εr is taken to equal unity. In reality these insulations have relative permittivity in the range ε_r = (3 ... 4). At the end of the simulation, an approximate method to correct for this systematic error is proposed.

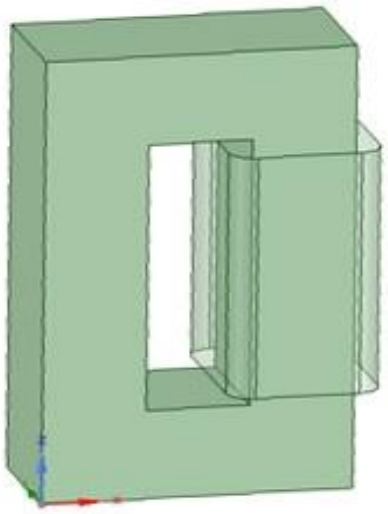

Fig. 6.3. Diagram of the magnetic core of the transformer with the protective shield

6.3.3. USING COMSOL TO DETERMINE SHIELD CAPACITANCE

The determination of the screen capacitance is done assuming that the integration domain is linear. In the COMSOL , the problem of determining the shield capacitance can be approached by a method which involves setting the shield potential to a certain value U and

using numerical methods specific to the software to determine the value of the electric charge Q on the shield and the value of the electrostatic field energy We.

The value of the imposed electrical voltage U is chosen randomly, since, the domain being linear, the value of the capacitance does not depend on its value. In this case, it is assumed, for example, that the value of this voltage is U = 100 V.

When solving the problem numerically, the refinement of the integration network is of great importance. Two variants were used to solve the problem. In the first variant a rough refinement network was used, and in the second variant a finer network was used, obtained automatically by the COMSOL program through three successive refinement steps, depending on the areas of the integration domain where the quantities have a smaller or larger variation.

Finally, the values of the electrical capacitance of the shield are obtained, calculated by imposing a value of 100 V for the electrical voltage.

The following values were obtained for the rough mesh refinement network of the calculation domain:

- C = 38.2 pF, if the defining relation applies ($C = \frac{Q}{U}$)
- C = 32.96 pF, if the energy relation applies ($C = \frac{Q^2}{2W_e}$)

The following values were obtained for the fine mesh refinement network of the calculation domain:

- C = 37.83 pF, if the defining relation applies ($C = \frac{Q}{U}$)
- C = 35.15 pF, if the energy relation applies ($C = \frac{Q^2}{2W_e}$)

It is found that the refinement mode of the calculation domain has an influence on the numerically calculated values of the shield capacitance. The capacitance values calculated with the relations ($C = \frac{Q}{U}$) and ($C = \frac{Q^2}{2W_e}$) differs by about 13.71% when considering the mesh refinement network and by about 7.08% when considering the fine mesh refinement network. It is obvious that the values obtained for the two cases are different due to the integration errors in the case of the two refinement network used in the calculation. From a

theoretical point of view the values of the screen capacitance are the same regardless of the method used.

6.3.4. CORRECTION OF SHIELD CAPACITANCE VALUES

In the previous paragraphs the presence of dielectric zones inside the transformer window was ignored. In the case of the transformer studied, there are also regions in the window where dielectric is found, such as the hostaphane insulations between the layers of the windings, with equivalent thickness $d_1 = 0.8$ mm and the voltaflex insulations between the windings and between the windings and the screen with equivalent thickness $d_2 = 1.2$ mm. Hostaphane has relative electrical permittivity $\varepsilon_{r1} \approx 3.5$ and voltaflex has relative electrical permittivity $\varepsilon_{r2} \approx 3.8$.

To determine the capacitance correction factor of the shield, the flat capacitor model is proposed and not the cylindrical one like the shield. This assumption does not significantly influence the results, since the correction factor is a dimensionless quantity whose value changes very little when switching from the cylindrical to the planar capacitor.

Therefore, the error that is made in the calculation of the shield capacitance if the insulations in the transformer window are removed is about 3 percent, the shield capacitance is about 3 percent higher than the value resulting from the numerical calculation in COMSOL.

CHAPTER 7

PROTECTION OF ELECTRICAL TRANSFORMERS AGAINST LIGHTNING OVERVOLTAGES USING ARRESTERS

7.1. INTRODUCTION

Transformer substation equipments are protected against direct lightning strikes using lightning rods, and also against surge voltages propagating from high-voltage lines using surge arresters.

7.2. SURGE ARRESTER

Surge arresters are equipment in the category of devices for protection against voltage faults. This equipment is classified according to design variants such as [16]:

(a) Variable resistance surge arresters with priming spark gaps and shunt resistors (VRA);

b) Metal oxide surge arrester without priming spark gaps (MOA).

7.2.1. VARIABLE RESISTANCE SURGE ARRESTERS

The variable resistance surge arrester reduces the value of overvoltages through voltage-dependent non-linear resistors to a value equal to the protection level.

The construction of a variable resistance surge arrester and the schematic circuit diagram are shown in Fig. 7.1. The active part of the surge arrester consists of the shunts 1 and the variable-resistance shunt resistors 2. These consist of several silicon carbide discs of special construction and suitable composition [17]. The whole construction is protected by the porcelain cover 3, and the metal end caps 4 act as sealing of the construction and at the same time act as connection terminals [16].

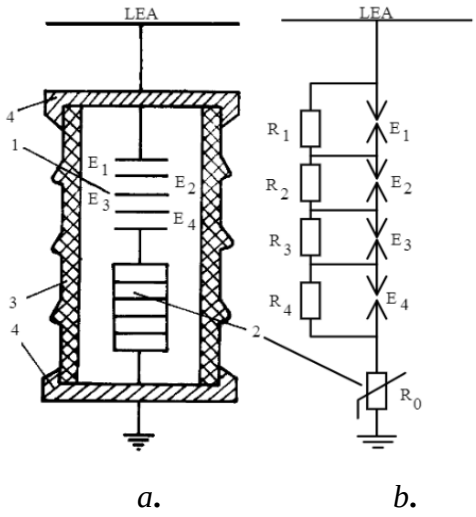

a. *b.*

Fig. 7.1. Variable resistance surge arrester (*a*); Electrical diagram (*b*) [17]

Shunt resistors, R_1, R_2, R_3, R_4, are an integral part of the silicon carbide surge arrester with spark gaps and have a very high value, ensuring that the surge is evenly distributed over the arrester spark gaps.

7.2.2. METAL OXIDE SURGE ARRESTER

Fig. 7.2 shows the section of the zinc oxide surge arrester without spark gaps and with a single column of ZnO blocks [18].

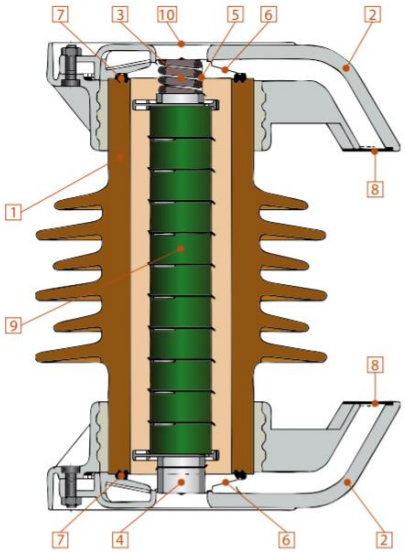

Fig.7.2. Zinc oxide surge arrester section [18]

The flanges 10 are cemented to the porcelain housing 1 and include the sealing device. The sealing device at each end of each unit consists of a pre-stressed stainless steel plate 6 with a rubber gasket 7. This serves to fix the column of ZnO blocks 9 in the longitudinal direction by means of springs 3 and copper plates 5. The ionised gases cause a fast increase in internal pressure, which in turn causes the sealing plate to open and the ionised gases to escape through the venting ducts 2. The lower part also contains desiccant 4 which has the property of absorbing moisture. The nameplate 8 shows the main characteristics of the surge arrester.

The main advantages of metal oxide surge arresters are as follows:

- From a construction point of view, they have a small size and high fiability by removing the spark gaps and equalising resistors;
- The voltage-time protection characteristic of the surge arresters is stable;
- Protection is about 20% higher than with conventional construction technology [19].

7.2.3. SURGE ARRESTER FAILURE

The main causes of surge arrester failure are: moisture due to improper arrester sealing, external explosion, excessive partial discharges, atmospheric overvoltage, temporary overvoltage, overload which can occur if surge arresters are subjected to overvoltages generated by switching capacitor banks, switching or powering long lines, switching high voltage lines, ageing of discs, external contamination, unbalanced electric field, incorrect

alignment of disc column, improper arc pressure, mechanical stress, insufficient dielectric strength.

According to the operating specifications of surge arresters, the failure rate of surge arresters is 0.005%/year.

7.2.4. CURRENT STATUS AND FUTURE DEVELOPMENTS

The latest developments in the field of high-voltage surge arresters are driven by the need to increase safety and reliability. Current concerns involve the following elements:

- excessive height (for example, more than 10 m), leading to axial unbalance effects of voltage, power and temperature, in addition to mechanical problems;

- low level of required switching impulse protection, leading to high power management requirements;

- high number of metal oxide resistors requiring very low probability of failure of individual units during power injection;

- limited protective distance, as part of the normally provided protective distance is actually used by the surge arrester.

Improvements in the technical characteristics of surge arresters are reduction in their size for the same voltage level. Manufacturers such as Meidensha [20] report a reduction in surge arrester volume of up to 44% due to these changes.

7.3. LIGHTNING RODS

Another type of lightning protection to absorb direct lightning strikes is the lightning rod. One characteristic of lightning is that it is more likely to strike the tallest objects, so vertical metal lightning rods are installed in a power station on the frame poles, and are between 3 m and 9 m high depending on the voltage level of the station.

Another type of lightning rod called a dissipation system prevents direct lightning strikes by reducing the electric field below the lightning strike level inside the protected area. The diversity of lightning dissipation systems and their applications has increased in various areas such as: poles, power transmission and distribution lines, flat-roofed industrial and commercial buildings, conical-roofed storage tanks used in the petrochemical and flammable storage industries, industrial chimneys/exhaust stacks, industrial and commercial tethered structures, cable cars.

Active or ionizing lightning rods are another model of protection against direct lightning strikes equipped with an electro-pulse generator that emits electrical pulses that are in reserve when there is no storm, and activate when there are thunderstorm conditions.

The lightning current passes through the outside of the external casing and through the free space to be conducted to ground without damaging the internal circuitry.

CHAPTER 8
OVERVOLTAGE PROTECTION OF ELECTRIC POWER TRANSMISSION LINES

8.1. INTRODUCTION

Thunderstorms with lightning are very dangerous. The frequency of thunderstorms on earth every day is 4000 storms and 9 million lightning strikes at the same time. [21]

According to a report on the achievement of performance indicators for electricity supply services [22], 694 incidents were recorded in the category of special incidents reported in the year 2020 in the concessionary Distribution Operators (DOs).

A significant percentage of 15.5% of faults due to extraordinary weather conditions is observed, including lightning overvoltages.

8.2. METHODS OF PROTECTING OVERHEAD POWER LINES AGAINST OVERVOLTAGES

The following describes methods of protecting overhead power lines against atmospheric and switching overvoltages.

1) Appropriate choice of power line route (keraunic index)

Site/route selection is the first consideration for overhead power lines as well as power stations, wind farms [23] and photovoltaic, nuclear and thermal installations. There is a keraunic parameter and a keraunic map that determine the annual frequency of lightning strikes. The keraunic parameter, the Nk index defines the average number of days in a year with lightning strikes in an area.

Electrical discharges between/in between clouds do not reach the earth's surface and occur most often during storms and are about 85%. Lightning strikes in contact with the ground or various objects account for a smaller percentage, about 15% in atmospheric phenomena with thunderstorm character, but their impact is severe.

The average lightning density calculated from 2016 to 2021 on a scale of events/km²/year ranks Gorj county first with the most events, with a total of 11.3 events/km²/year.

All these data collected from the monitoring of storm activities are necessary in the design of power plants to ensure the best protection against atmospheric surges.

2) Protective conductors

Protective conductors are a technical measure against lightning surges, so they are mounted on the top of the poles, above the active conductors.

Protective conductors or guard wires are used to equip the OHL and are two types: classic or FO (fibre optic).

3) Earthing sockets

The earthing socket is intended to dissipate electrical charges resulting from electrical discharges without causing dangerous step surges.

Earthing sockets are designed to ensure electrical continuity.

4) Chains of insulators

Insulator chains are components of overhead power lines, which are used to electrically insulate active conductors from earth and to fix them to poles.

Clamps and fittings are parts that connect the line conductors, insulators and poles of overhead power lines. Clamps make direct contact between insulators and conductors, and fittings join insulators to pole brackets or between insulators and clamps.

5) Rapid automatic restart (RAR)

Overhead power lines are often subject to faults and are de-energised, and then after a short time in which the fault is neutralised the RAR device comes into operation which checks that the safety conditions are met and performs rapid automatic reclosing, and the OHL will operate in normal safe conditions.

An RAR equipment has a main device, namely a circuit breaker, which trips when a fault such as an atmospheric surge occurs on the overhead power line.

6) Special protection of line crossings

At overhead power line crossings, overhead power line crossings over motorways and high frequency roads the risk of atmospheric surges affecting other overhead power lines is increased. The following design provisions may be considered:

- compliance with the minimum distances required between circuits;
- choosing network elements with high mechanical resistance such as: elevated poles, double insulator chains, reduction of spans between poles, reduction of the crossing angle, reduction of the protection angle.

7) Surge arresters on overhead power lines

The installation of arresters on overhead power lines ensures the protection of the power grid against lightning and switching surges, thus increasing the reliability of the whole system.

According to an ABB study [18], Fig.8.1 shows the effect of arresters on the evolution of overvoltage on a 550 kV, 100 km long power line that was reconnected following a fault. Thus, on the graph with continuous line the unit value of the overvoltage over the whole length of the OHL without arresters is shown, with broken line the OHL overvoltage protection with arresters mounted at the ends of the line was represented, and with dotted line the protection with arresters at the ends of the line and supplemented with two intermediate arresters per line.

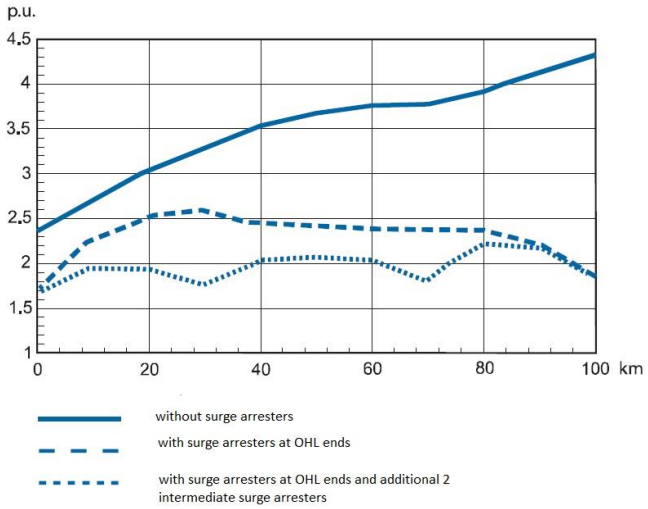

Fig.8.1. Graphical representation of the evolution of overvoltage on the 550 kV LEA with and without line Arresters installed [18]

In conclusion, the graphical representation in Fig. 8.1 shows the improvement of the overvoltage value using line arresters as a protection method.

CHAPTER 9
CONCLUSIONS AND ORIGINAL RESULTS

9.1. GENERAL CONCLUSIONS

In this doctoral thesis, lightning overvoltages in general and their consequences have been analysed with a focus on the analysis of several possibilities: propagation of overvoltages along electrical equipment, especially electrical transformers, but also overhead power lines. At the same time, the means of protection against these overvoltages and the equipment used for this purpose were analysed. Of particular theoretical and practical interest is the behaviour of high-power electrical equipment to impulse overvoltages, which are applied at the input terminal of high-voltage winding for electrical transformers, and for power transmission lines the interest is in improved means of protection. The study of transient processes at impulse voltage leads to the correct choice of transformer winding insulation and power line insulation from both a functional and an economic point of view.

Chapter 1 of the paper analyses a consistent classification of overvoltages, showing that several criteria are proposed in the technical literature such as: their shape and duration, the size of the overvoltage wavefront. It reviews the negative effects of overvoltages (lightning and lightning strikes) and how they act on people, buildings or tall objects in the area (poles, trees) and gives some examples from oil refineries, storage sites for flammable substances and aircraft in the surge zone. The historical treatment of atmospheric overvoltage problems propagating along the high voltage windings of electrical power transformers worldwide is reviewed. At the end of Chapter 1 the issue of power quality in each phase of generation, transmission, distribution and supply is addressed. Thanks are expressed to those who assisted the author during the preparation of this PhD thesis.

Chapter 2 of the paper describes the main electrical schemes of transformers exposed to lightning overvoltages, showing that these schemes are totally different from the equivalent schemes used in the normal operating regimes of these transformers. The frequency of the lightning overvoltage front is very high and because of this, capacitances appear in the equivalent scheme. On the other hand, for good accuracy, resistors and inductances must also be included in the equivalent scheme. Both equivalent schemes at overvoltages where parameters defined per unit length appear and equivalent schemes with lumped parameters are considered.

Chapter 3 presents lightning impulse modelling for testing transformer windings. At the beginning, the determination of the parameters of a pulse generator that generates a surge waveform as close as possible to the waveform presented in the standards is considered. The entry of overvoltages at the input terminals of transformer windings and their propagation along these windings is accompanied by significant stresses on the insulation between winding turns, on the insulation between windings and ground, and on the insulation between windings. The time-varying shape of the lightning wave is defined, then the surge wave is modelled in LTspice so that it is as close to the standard shape, with good agreement between the standard waveform and the modeled waveform.

In ***Chapter 4*** the simulation of lightning impulse propagation in the high voltage winding of a single-phase electrical transformer is analysed. It is shown that transformers are not damaged due to transient or switching surges, but due to lightning overvoltages. The methods presented in the technical literature for determining the parameters of electrical transformers subjected to atmospheric overvoltages are reviewed, showing that the most commonly used are methods based on numerical simulation of electrical circuits, because at very high lightning wavefront frequencies, experimental methods or analytical methods cannot be easily applied. The use of LTspice software for transient regime analysis offers a major advantage in terms of computational time and changing different parameter values to quantify the weight of each parameter in the final result is relatively easy.

Chapter 5 deals with the influence of varying the parameters of the equivalent transformer scheme on the propagation of overvoltage waves along the high voltage winding. Lightning pulses penetrate the transformer windings and result in a complex transient process. It is shown that the penetration of overvoltage voltages inside the transformer can destroy the insulation between the transformer windings, or between the windings and the ferromagnetic core, or between the windings and the transformer's metal casing. Starting from the reference values R_{0L}, R_{0T}, L_{0L}, C_{0L} and C_{0T} of the parameters of the equivalent scheme, the influence of the variation of each of the five parameters of the equivalent scheme under the hypothesis of variation of the values of one parameter, the other four remaining constant at their reference values, is studied one by one by modelling in LTspice. In this way, the influence of each of the 5 parameters on the maximum values of the overvoltages occurring along the high voltage winding of the transformer is studied in turn. At the end of the chapter some conclusions are drawn: the most stressed part of the transformer high voltage winding is the last section of the winding; of the five parameters appearing in the equivalent scheme, the greatest importance is

given to the values of the transverse capacitance C_T and the longitudinal capacitance C_L; less importance in the equivalent scheme is given to the parameters R_L, L_L and R_T in the equivalent scheme.

Chapter 6 discusses how the guard ring and protective shield serve to mitigate lightning overvoltages. The guard ring has the advantage that it mitigates the initial shock due to the atmospheric overvoltage wave front in the sense that the overvoltage wave is more evenly distributed along the high voltage winding and helps to provide dielectric protection for the incoming turns of this winding. In the case of the guard ring, 4 calculation hypotheses are analysed and for each hypothesis the time variation curves of the overvoltages propagated along the high voltage winding are plotted. Another problem dealt with in Chapter 6 concerns the determination of the surge protection screen capacitance for the electrical transformer. The COMSOL software is used to determine this capacitance using two methods of grid refinement, namely a rough mesh refinement and a fine mesh refinement. It is shown that the differences in the two cases are not significant, with the conclusion that more accurate results are obtained with the finer mesh refinement.

Chapter 7 of the paper is concerned with the protection of electrical transformers against lightning overvoltages using surge arresters. Equipment in electrical transformer stations is protected against direct lightning strikes using surge arresters and lightning rod. The level of protection provided by surge arresters depends on the distance from the equipment to be protected, its location upstream or downstream, the performance of the surge arrester, the configuration of the substation and the characteristics of the power line. Lightning rod have the property of taking direct lightning strikes and are useful for protecting objects higher than the ground.

Chapter 8 looks at how to protect power transmission lines from overvoltages. It is shown that these overvoltages can be caused directly by lightning strikes, or can occur as a result of switching overvoltages or induced surges. Measures to protect against atmospheric overvoltages and overhead power line switching overvoltages are methods of safety in operation with impact on humans and equipment that may be damaged. Some methods of protection of overhead power lines against atmospheric and switching overvoltages are also presented such as: proper choice of power line routing, provision of line with protective conductors, earthing sockets, line surge arresters and activation of rapid automatic reclosing (RAR) when appropriate.

9.2. ORIGINAL CONTRIBUTIONS

The PhD thesis deals a topic which grows in interest, dealing with the protection against lightning overvoltages of electrical equipment and the power lines to which this equipment is connected.

The main original contributions of the PhD thesis are the following:

- A compact and well-documented presentation of the classification of overvoltages, their negative effects and the quality criteria for electricity produced in power plants;
- A synthesis of the schemes of electrical transformers at atmospheric overvoltages, both for parameters defined per unit length and lumped parameters;
- Modelling the lightning impulse by numerical methods so that its time-varying shape is as close as possible to the standard shape, with the shape falling within the permissible error range.
- Study of the influence of the variation of the parameters of the transformer equivalent diagram to atmospheric overvoltages, on the maximum values of the overvoltages propagating along the high voltage winding in order to reduce these maxime.
- Analysis of the influence of the guard ring on the maximum values of the overvoltages in the sense of decreasing these maxima, using numerical modelling methods in LTSpice.
- Determination of the overvoltage protection shield capacitance of electrical transformers using finite element numerical methods, using two numerical calculation methods: calculating the electrical load on the armatures of the capacitor with which the protection screen is equated, and calculating the electrical energy stored in the equivalent capacitor;
- Well-documented analysis of the use of electrical surge arresters to protect power lines against lightning overvoltage, and detailed description of the most commonly used types of surge arresters;
- Study of the protection of electric power transmission lines against overvoltages and protection measures currently used in the energy industry.

9.3 PERSPECTIVES FOR FURTHER DEVELOPMENT

- Determination of the capacitance of the guard ring for overvoltage protection of the electrical transformer by finite element numerical methods, methods analogous to those used in the calculation of the capacitance of the protective shield;
- Analysis of the influence of the protective shield on the maximum values of the overvoltages in the sense of decreasing these maximum values, using numerical modelling methods in the LTspice calculation environment;
- Writing special chapters and publishing them as books and scientific papers on lightning overvoltage protection of electrical power equipment and power transmission lines;
- Obtain practical information on overvoltage protection systems for electrical equipment and collaborate with various companies in this field to carry out specific projects.

SELECTIVE BIBLIOGRAPHY

[1] *Ghid de Aplicare - Calitatea Energiei Electrice*, SIER / European Copper Institute, 2001.

[2] Ciumbulea Gloria, Deleanu S., Iordache M., Curteanu S., Galan N., Moscu A., *Computation Overvoltage Distibution Across the High Voltage Winding of the Electric Power Transformer*, The 10th INTERNATIONAL CONFERENCE ON ELECTROMECHANICAL AND POWER SYSTEMS, Oct. 2015, Chișinău, Rep. Moldova.

[3] Deaconu, I.D., Chirilă, A.I., Năvrăpescu, V., **Răchițeanu Alina**, Viișoreanu, A.M. Ghiță, C., Sărăcin, Gabriela, *Lighting impulse voltage modeling for transformer windings testing*, The 11th International Symposium on ADVANCED TOPICS IN ELECTRICAL ENGINEERING – ATEE, 2019, Bucharest, Romania, DOI: 10.1109/ATEE.2019.8724942 , Conferință ISI.

[4] IEC 60060 – 1 « *High – voltage test techniques – Part 1 – General definitions and test requirements »*, International Electrotechnnical Commission, Sept. 2010, Edition 3.0.

[5] IEC 60060 – 2 « *High – voltage test techniques – Part 2 – Measuring systems*», International Electrotechnnical Commission, nov. 2010, Edition 3.0.

[6] *Impulse Voltage Generator Test System*, [Online] http://www.bhthv.com/products /Impulse_voltage_generator_test_system.html, [Accesat ianuarie 2019]

[7] Swaffield D.J., Lewin P.L., Dao N.L., Hallstrom J.K., *Lightning impulse wawe-shapes: defining the true origin and it's impact on parameter evaluation,* https://www.researchgate.net/publication/39995505

[8] *Analog Devices, LTspice,* Simulation Software,, 2019 [Online], "https://www.analog.com/en/design-center/design-tools-and-calculators/ltspice-simulator.html.

[9] Erwin M. O., *Versuche über die Prüfung von Isolatoren mit Spanningsstößen,* Elektrotechnische Zeitschrift, 25, pp. 652–654, 1924.

[10] Deaconu I.D., Chirilă A.I., Năvrăpescu V., Ghiță C., **Răchițeanu Alina**, Viişoreanu A.M., *The Influence of Parameters of a Power Transformer Winding Equivalent Distributed Circuit Model on Atmospheric Overvoltage Wave Internal Propagation along the Windings*, EPE 2020 Iasi – The 11th International Conference and exposition on electrical and power engineering, 2020, DOI: 10.1109/EPE50722.2020.9305584, Conferință ISI.

[11] Viişoreanu A.M, **Răchițeanu Alina,** *Reliability and maintenance of wind power systems,* EMERG, Volume VI, Issue 3/2020, ISSN 2668-7003, ISSN-L 2457-5011, Bucharest, Romania, DOI: 10.337410/EMERG, The EMERG publication is BDI indexed in EBSCO and Copernicus International.

[12] **Răchiţeanu Alina,** Viişoreanu A. M., *Propagarea undelor de supratensiune în transformatoare prevăzute cu inel de gardă*, Simpozionul de Masini Electrice - SME '21, Ediţia a XVII-a, Bucuresti, 2021, ISSN / ISSN-L: 1843-5912, Journal.iem.pub.ro/apme/, https://www.doi.org/10.36801/apme.2021.1.5

[13] Bălă C., *Maşini electrice*, Editura Didactică şi Pedagogică, Bucureşti, 1979, 632 pg.

[14] Deaconu I.D., Chirilă A.I., Ghiţă C., NăvrăpescuV, **Răchiţeanu Alina**, Viişoreanu A.M., Popescu S.V., Gheorghiu Corina - Ioana, Sărăcin Cristina - Gabriela ,*Determination of the Electric Capacitance of the Overvoltage Protective Shield of an Electric Transformer*, The 12th International Symposium on ADVANCED TOPICS IN ELECTRICAL ENGINEERING – ATEE, 2021, Bucharest, Romania, DOI: 10.1109/ATEE52255.2021.9425086, Conferință ISI.

[15] COMSOL Multiphysics - Understand, Predict, and Optimize Physics-Based Designs and Processes [Online] https://www.comsol.com/comsol-multiphysics. [Accesat ianuarie 2021]

[16] **Răchiţeanu Alina**, Viişoreanu A.M., *Overvoltage protection of transformers and high voltage networks by surge arrester*, EMERG, Volume VI, Issue 2/2020, ISSN 2668-7003, ISSN-L 2457-5011, Bucharest, Romania. DOI: 10.337410/EMERG, The EMERG publication is BDI indexed in EBSCO and Copernicus International.

[17] Adam M., Baraboi A., *Echipamente electrice II*, Editura Gh.Asachi, 2002.

[18] ABB guide, , *Hight Voltage Surge Arresters Buyer´s Guide*, 2009

[19] **Răchiţeanu Alina**, Viişoreanu A.M., *Surge arrester for protection against overvoltage of high voltage networks*, EMERG, Volume VI, Issue 3/2020, ISSN 2668-7003, ISSN-L 2457-5011,

Bucharest, Romania, DOI: 10.337410/EMERG, The EMERG publication is BDI indexed in EBSCO and Copernicus International.

[20] Meidensha Corporation, *Stage7: Protecting the Power Grid from the threat of Lightning Strikes*, [Online] https://www.meidensha.com/knowledge/know_10/hitotech/stage7/, [Accesat: aprilie 2022]

[21] *Consequences of overvoltages*, Aplicaciones Tecnologicas Lighting & Earthing, [Online] https://at3w.com/en/ , [Accesat noiembrie 2021]

[22] *Raport privind realizarea indicatorilor de performanţă pentru serviciile de transport, de sistem şi de distribuţie a energiei electrice şi starea tehnică a reţelelor electrice de transport şi de distribuţie (2020)* – ANRE, [Online] https://www.anre.ro/ro/energie-electrica/rapoarte/rapoarte-indicatori-performanta , [Accesat ianuarie 2022]

[23] Viişoreanu A.M., **Răchițeanu Alina**, *Evaluation of wind potential from a location and layout of the turbines*, Simpozionul de Masini Electrice, Ediţia a XVII-a, Bucuresti, 2021, ISSN/ISSN-L:1843-5912, Journal.iem.pub.ro/apme/, https://www.doi.org/10.36801/apme.2021.1.10